BNL-220683-2020-JAAM

Low-temperature proton irradiation damage of isotropic nuclear grade IG-430 graphite

N. Simos, S. Ghose

To be published in "JOURNAL OF NUCLEAR MATERIALS"

December 2020

Photon Sciences

Brookhaven National Laboratory

U.S. Department of Energy

USDOE Office of Science (SC), Basic Energy Sciences (BES) (SC-22)

Notice: This manuscript has been authored by employees of Brookhaven Science Associates, LLC under Contract No. DE-SC0012704 with the U.S. Department of Energy. The publisher by accepting the manuscript for publication acknowledges that the United States Government retains a non-exclusive, paid-up, irrevocable, world-wide license to publish or reproduce the published form of this manuscript, or allow others to do so, for United States Government purposes.

DISCLAIMER

This report was prepared as an account of work sponsored by an agency of the United States Government. Neither the United States Government nor any agency thereof, nor any of their employees, nor any of their contractors, subcontractors, or their employees, makes any warranty, express or implied, or assumes any legal liability or responsibility for the accuracy, completeness, or any third party's use or the results of such use of any information, apparatus, product, or process disclosed, or represents that its use would not infringe privately owned rights. Reference herein to any specific commercial product, process, or service by trade name, trademark, manufacturer, or otherwise, does not necessarily constitute or imply its endorsement, recommendation, or favoring by the United States Government or any agency thereof or its contractors or subcontractors. The views and opinions of authors expressed herein do not necessarily state or reflect those of the United States Government or any agency thereof.

Low-temperature proton irradiation damage of isotropic nuclear grade IG-430 graphite[1]

N. Simos[a,*], P. Hurh[c], N. Mokhov[c], M. Snead[b], M. Topsakal[a], M. Palmer[a], S. Ghose[a], H. Zhong[a], Z. Kotsina[d], D.J. Sprouster[b,*]

[a] Brookhaven National Laboratory, Upton, NY 11973, USA
[b] Stony Brook University, Stony brook, New York, 11784, USA
[c] Fermi National Laboratory, Batavia, IL 60510-5011, USA
[d] National Center for Scientific Research, Demokritos Ag., Paraskevi 15310, Greece

A B S T R A C T

IG-430, a fine-grained, isotropic graphite grade is a promising candidate for the future Very High Temperature Reactors (VHTR). IG-430 which provides higher density, strength, and thermal conductivity, has already been developed as a graphite for next-generation HTGR, and is expected to be employed. This graphite grade, however, is lacking enough database that is needed for design. The present study aims to enhance the database with experimental data focusing on the low temperature regime (90–210 °C) by using 120–200 MeV protons to irradiate the IG-430 graphite to peak fluence of ~1.2 10^{25} m^{-2}. It is anticipated that radiation-induced changes in the graphite properties and damage to be more pronounced in this low temperature regime than in elevated temperatures where damage annealing is taking place simultaneously. IG-430 graphite was characterized following irradiation for mechanical property changes (modulus and strength), dimensional stability and irradiation-induced growth as well as microstructural changes using high energy X-rays and different X-ray diffraction techniques. In assessing proton irradiation effects on the IG-430 graphite grade, comparison of radiation effects was made with the IG-43 grade, the un-purified version of IG-430, as well as other isotropic graphite grades. IG-430 was shown in this study to be better graphitized than other isotropic graphite grades. The study also revealed that during proton irradiation at low temperatures (~100 °C) the IG-430 exhibits stored energy release.

1. Introduction

IG-430, a pitch coke, isostatically molded, purified fine grain, isotropic (10–20 μm) nuclear-grade graphite produced by Toyo-Tanso (Osaka, Japan) is considered a candidate for the future VHTR reactors. It has already been developed as a graphite for next-generation HTGR and is expected to be employed. The IG-430 grade offers higher density, strength, and thermal conductivity but it is lacking the database, or the breath of experimental data needed for implementation in the design of HTGR or VHTR. To-date IG-110 is the world's only graphite material employed forming components in high-temperature gas-cooled reactors (HTGR). Towards the objective of IG-430 use in next generation high temperature gas-cooled reactor [1] material properties of IG-430 graphite grade were evaluated and compared to IG-110 graphite currently the leading candidate for in-core components of VHTR. IG-430, exhibiting higher tensile, compressive and fatigue strength and resistance to oxidation than IG-110 is an advanced candidate for the VHTR. Several other studies [2–4] generated and reported irradiation data for new graphite grades including IG-430. In [5] 3 MeV C+ irradiation effects on the microstructure, mechanical properties and oxidation of IG-110 and IG-430 nuclear graphites were studied and compared revealing that the size of Mrozowski cracks to be larger in the IG-110 than the IG-430 prior to irradiation. The changes in the crystallinity and the crystallite size appeared larger for the IG-430 and the IG-110, respectively as a result of ion irradiation. As part of a European R&D programme [6] on nuclear graphite, several grades including IG-430, were irradiated to high neutron doses (8 dpa) and at 750 °C temperatures and tested in post-irradiation for on dimensional changes, dynamic Young's modulus, coefficient of thermal expansion and coefficient of thermal conductivity. Towards the goal of identifying applicable

[1] *This article is dedicated to the loving memory of our friend and colleague Nikolaos Simos, a true pioneer of the field of radiation damage in materials and main author of this article, who suddenly passed away on 15th of July 2020. He will be dearly missed.*

* Corresponding authors.
E-mail address: david.sprouster@stonybrook.edu (D.J. Sprouster).

graphite grades for Generation-IV nuclear reactor applications, fine-grain nuclear graphite grade G347A has been irradiated and studied [7] for property changes that occur at high neutron fluences 40 10^{25} n/m^2 [E > 0.1 MeV] and temperature ranges 290–800 °C. Noteworthy observations in [6,7,9] were the anisotropic behavior of dimensional change in an otherwise isotropic graphite and the parabolic fluence dependence of Young's modulus change.

Proton irradiation-induced creep of POCO ZXF 5Q 70 μm-thick graphite was studied in [8] using low energy protons from a 1.7 MeV Tandetron accelerator. Dose rate effects in combination with high temperatures, 700 °C to 1200 °C range, were investigated leading to the conclusion that proton irradiation-induced creep appears to exhibit linear dependence with dose rate and temperature and no dependence on accumulated dose. The role of γ-ray annealing of radiation defects during in-reactor irradiation was identified as the reason for observed order of magnitude higher creep compliance induced by protons in [8] even though both irradiations 1.7 MeV protons and in-reactor neutrons) showed linear dependence of creep rate on dose rate and temperature. It was concluded [8] that based on the similarity in creep behavior and microstructural changes that proton irradiation may serve as a valuable tool towards understanding in-reactor creep in graphite. Relevant to the present study involving high energy protons and bulk samples, it is concluded/recommended in [8] that for suitable comparisons between proton and in-reactor irradiation effects of nuclear graphite grades such as IG-110 (closely related to IG-430 of this study), higher proton energies that in turn permit the study of thicker, mm-size samples instead of μm-size would be required.

As part of the INNOGRAPH irradiation campaign several graphite grades, including IG-110, considered for High Temperature Reactors were irradiated at 750 °C and 950 °C [9] aiming to also address scatter in material properties and their evolution under irradiation as well as comparison between grades. It was concluded in [9] that coarse grained grades exhibited lower dimensional anisotropy and fracture toughness. A new model for the response of graphite to neutron irradiation has been proposed in [10] where damage undergoes a change at ~250 °C. In this model, and for irradiation temperatures below ~250 °C particle a permanent, nano-buckling of the layers is taking place. Above this threshold temperature, layers fold, forming what is termed in [10] "ruck and tuck defect". First principles and molecular mechanics calculations results were used in [10] to support the model which, contrary to the widely accepted graphite damage mechanisms based on atomic displacements, predicts little or no evidence of the growth of new sheets from the aggregation of interstitial atoms, therefore questioning dimensional changes and energy storage in irradiated graphite, which invoke point defect aggregation into new basal planes.

IG-430 graphite has attracted the interest of next generation, multi-MW power particle accelerators as a low-Z pion-generating target capable of surviving thermal shock that is compounded by prolonged exposure and damage. Several multi-MW particle accelerator initiatives such as the Neutrino Factory, Neutrino Superbeam, and the Long Baseline Neutrino Facility (LBNF) [11–13] have considered the IG-430 grade as a potential target material. Such interest has prompted several irradiation campaigns using energetic protons with objectives (a) assessing whether surrogate irradiating particles to neutrons (i.e. energetic protons at less fluence but higher damage rate) (b) understanding changes in physical and mechanical properties as well as microstructure that occurred as a result proton fluence. Establishing such correlation in damage may prove to be extremely useful in design at extreme reactor conditions.

In both initiatives, VHTR and multi-MW next generation accelerators, the changes occurring in the physio-mechanical properties of the graphite material as a result of long exposure to energetic irradiating particles, i.e. fast neutrons, or protons, need to be fully understood. While the correlation of the damage induced in graphite, IG-430 or any other grade, from protons or fast neutrons may not yet be fully understood, the experimental data to-date [12–14] provide evidence of damage similarities on the basis of fluence. Consequently, the large body of work on irradiated graphite generated to-date addressing the physio-mechanical changes on several graphites may come into play in evaluating the IG-430 grade The behavior of graphite under neutron irradiation has been explored over the past several decades in [15–25] In these studies, emphasis has been given to neutron-induced amorphization [18], dimensional changes [19,20,22] both macroscopic and lattice, swelling [21], Young's modulus and strength evolution [16,20,22], and thermal conductivity [23]. In [18] experimental evidence is reported that irradiation at 150 °C can produce large crystal dimensional changes in relatively small doses. Defect structures in nuclear grade graphite (NBG-18) under neutron and ion irradiation was studied in [25] concluding that even when irradiated to several tens of dpa, data indicate that the layered structure persists accompanied by the topological defects.

Stored energy release in post irradiation heating is addressed in [20,26–29]. Stored energy release represents an important consideration in the safe operation of reactor graphite moderators. Important work conducted at Brookhaven National Laboratory's research reactors in the 1960's and the establishment of activation energy for annealing interstitials in neutron irradiated graphite is presented in [27]. Ion and electron irradiation-induced defects and their migration in graphite, carbon interstitials and bonding with lattice atoms were studied in [30]. Using a correlation of X-ray diffraction and electron microscopy [31] two regimes of stored energy release were identified based on neutron fluence along with the critical dose of irradiation of ~6 10^{20} n/cm^2 at which on the (002) X-ray line broadens strongly and the energy release becomes shifted to higher temperature. The fluence threshold of 6 10^{20} n/cm^2 was interpreted as the critical fluence at which interaction of holes becomes appreciable so that the probability of the production of dislocation dipoles increases rapidly. Studies on graphite heavily irradiated with energetic protons [12,13] using X-ray diffraction have confirmed the presence of a similar threshold fluence beyond which the (002) diffraction line begins to broaden asymmetrically. Diffuse diffraction phenomena from neutron-irradiated single graphite crystals were reported in [32].

Irradiation induced deformations of graphite and carbon, including irradiation creep and post-irradiation annealing are discussed in [33] where a number of works on irradiated graphite used as moderator in reactors. Specifically, the effects of high neutron doses in reducing porosity introduced during manufacturing by graphite crystal growth resulting in the "tightening" of the aggregate structure, the rise in the elastic modulus and the partial recovery due to high temperature annealing are discussed based on experience and experimental data.

Swift heavy ions were used to irradiate high-density isotropic graphite [34] considered for a target and beam catchers, followed by high resolution X-ray post-irradiation evaluation. It was assessed in [34] from the X-ray diffraction that 3.6-MeV/u Au ions mainly induce disordering due to defect cluster formation and that at the stopping end of the ions, elastic collisions were assessed to be more effective than electronic excitation in inducing structural disorder. In [35] the oxidation of IG-110 and IG-430 graphite grades considered for core components of Very High Temperature Reactors were studies using ultrasound-based techniques and micro-indentation. Mrozowski cracks and oxidation behavior of IG-110 and IG-430 grades were explored in [36] reporting on higher oxidation rate of the IG-110 compared to IG-430 grade that may be attributed to the differences in the density and size of Mrozowski cracks which may originate in differences in the thermal

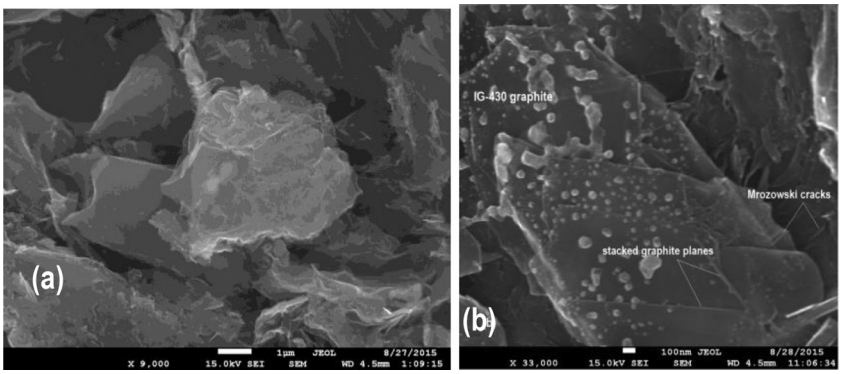

Fig. 1. (a) SEM micrograph of IG-430 at room temperature, (b) after annealing at 660 °C for 3 h. Noted presence of Mrozowski cracks and stacking of basal planes (grain size by Toyo-Tanso ~10 μm).

conductivity. Emulation of reactor irradiation damage using ion beams is discussed in [37].

In this study which focuses on the temperature regime 90–210 °C, several irradiation campaigns with energetic protons (120–200 MeV) were conducted at the Brookhaven Linear Isotope Producer (BLIP) facility [38]. The proton irradiations were augmented with a low temperature (T_{irr} ~80±10 °C, moderate fluence (~0.6 10^{20} n/cm^2, > 0.1 MeV, ~0.012 DPA) irradiation campaign which used spallation generated fast neutrons for comparative purposes. The peak fluence achieved in the proton experiments was ~10^{21} p/cm^2 (with irradiation temperatures varying between experiments between 90 and 200±10 °C).

Post-irradiation macroscopic and microscopic analyses was performed on the IG-430 graphite to assess whether surrogate irradiating particles to neutrons (i.e. energetic protons at lower fluence but higher damage rate) can provide crucial information on damage, particularly the low temperature regime, and to understand the changes in key physical and mechanical properties that occur as a result of proton irradiation. Specifically, effects on dimensional stability and changes in thermal expansion coefficient, post-irradiation annealing, irradiation-induced changes in mechanical strength and Young's modulus and their recovery through annealing. Changes in the IG-430 microstructure were evaluated using high energy X-rays with Energy Dispersive X-ray Diffraction (EDXRD) and X-ray Diffraction (XRD) techniques. For reference, IG-430 graphite is compared with the IG-43 grade for induced radiation damage from protons under similar conditions. IG-43 has preceded the interest in IG-430 for particle accelerator target applications which led to experiments and studies [15]. IG-43 is not considered a nuclear-grade graphite and it must be purified to become IG-430.

2. IG-430 pre-irradiation characterization

Unirradiated (as received) IG-430 graphite was analyzed using scanning electron microscopy (SEM), dilatometry and X-ray diffraction with high energy X-rays. Specifically, and using X-ray diffraction techniques such as EDXRD with 200 keV polychromatic X-rays, it was compared with other isotropic grades such as SGL R7650 and POCO ZXF 5Q to reveal the degree of graphitization.

Fig. 1 depicts SEM micrographs of unirradiated IG-430 for two states namely room temperature (Fig. 1a) and following thermal treatment at 660 °C (Fig. 1b). An average grain size of ~20 μm is estimated for IG-430 while Fig. 1b reveals the presence of impurities and Mrozowski cracks. The dimensional stability of IG-430 in the unirradiated state was studied using high precision dilatometry. Results are shown in Fig. 2 for thermal treatment up to 300 °C consisting of isotherms at 250 °C and 300 °C. For these temperatures, as seen in Fig. 2a, IG-430 dimensional change for 200 °C and 300 °C isotherms, the structure does not undergo any shrinkage indicating that there is no damage being recovered. Fig. 2b shows full dimensional recovery of the test sample upon completion of the thermal cycle.

Crystallographic analysis results deduced using 200 keV, polychromatic X-ray diffraction of several unirradiated isotropic grades (IG-430, POCO ZXF 5Q, SGL R7650) are shown in Fig. 3. It is evident, based on the narrower basal plane reflection (002), Fig. 3b, that IG-430 has been graphitized at higher temperature (2800 °C vs. 2500 °C for POCO ZXF 5Q) as shown from the narrower 002 reflection. Specifically, the d-spacing of IG-430 was measured to be d_{002} = 3.36814 Å compared to 3.3833 Å for POCO and 3.37944 Å for SGL R7650 respectively. The ideal graphite crystallite is characterized by d_{002} = 3.3354 Å.

2.1. Irradiation experiments

Several irradiation campaigns were conducted utilizing the 200 MeV proton Linac of the BNL accelerator complex [37] which currently can deliver in excess of 40 kW beam power. Specifically, and reported herein, two irradiation experiments using protons with energies in the range of 160–180 MeV were conducted reaching peak fluences of ~10^{21} p/cm^2 with irradiation temperatures in the range of 90–210±10 °C. The processes at these proton energies on graphite are elastic nuclear interactions, intranuclear cascades with protons and neutrons emitted with no pion or other new particle production. Evaporation with protons, neutrons, gamma, and light fragments (d, He^3, α) emitted. Spallation and de-excitation gammas in a final state and multiple Coulomb scattering. Electronic (ionization) energy loss is dominant for energy deposition. A small fraction of projectile energy goes to non-ionizing energy loss.

During the first irradiation campaign which explored the use of the IG-430 graphite as a pion production target material for the Neutrino Factory accelerator initiative [11] bar samples 42 mm long with a 3 × 3 mm^2 cross section were directly cooled with deionized water forced past the samples maintaining the peak temperature at T_{irr} ~90 °C. During the second irradiation campaign of IG-430 for the LBNF accelerator initiative the proton irradiation was conducted in argon atmosphere with the test samples arranged as shown in Fig. 4a. Specifically, the two types of samples (type-A and type-B) are tightly packed within the shown capsule in argon (front capsule window not shown) with the proton beam of Gaussian shape impinging normal to the plane as shown. The Gaussian shape of the proton beam results in a spatial variation of the fluence on the normal plane and, consequently on the irradiation temperature of each sample. Type-A samples in dog-bone

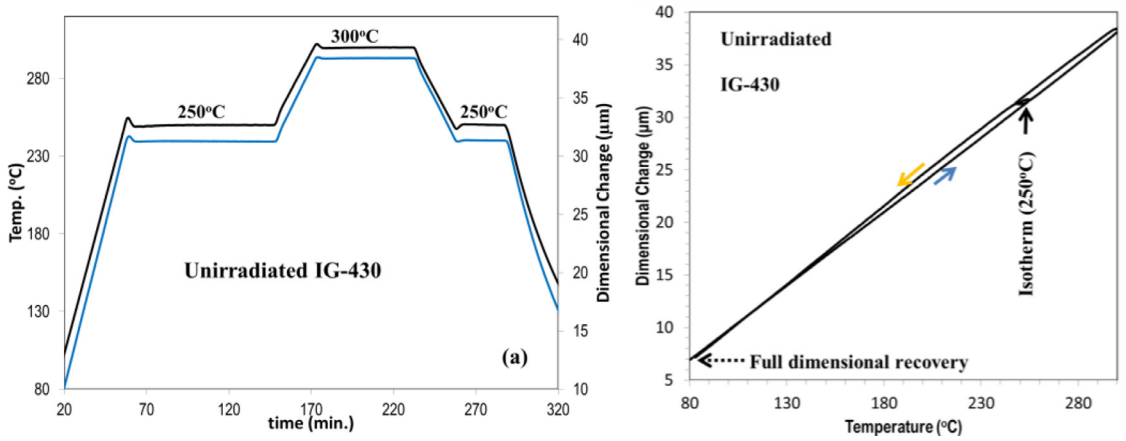

Fig. 2. (a) Dimensional stability of as-received IG-430 over isotherms, (b) dimensional recovery following thermal cycle treatment indicating low porosity in as-received IG-430.

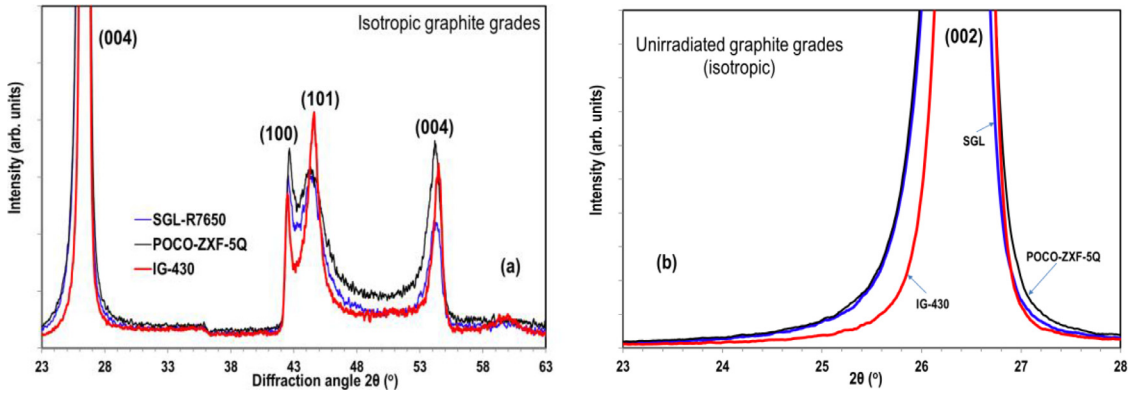

Fig. 3. Graphitization comparison of isotropic graphite grades based on X-ray diffraction.

shape are 42 mm long with 1mm thickness and 6 mm neck-down gauge. They are used for mechanical (stress–strain) testing and X-ray diffraction. Type-B samples are 29 mm long and 3 mm thick. They are used for thermal expansion coefficient (CTE) and volumetric changes, ultrasonic velocity changes and stored energy release. Details of type-A and type-B are shown in Fig. 4c and 4d respectively.

Fig. 4e depicts the IG-430 proton irradiation under argon atmosphere layout performed in tandem with the medical isotope production which is the primary purpose of the irradiation facility. For proton irradiation of the graphite, the energy of the Linac is increased from 118 MeV which is the normal operating energy during isotope production to 181 MeV and the graphite capsules are placed upstream of the isotope producing targets. The degradation of energy through the irradiated graphite must be precisely calculated to less than 0.5 MeV while the beam profile remains Gaussian with absolutely no shinning paths. To ensure that the beam degradation is uniform (no gaps between samples) in the array, the special shapes shown in Fig. 4c and d were adopted and precisely fabricated. Within each capsule, three layers of the 1 mm thick tensile samples are integrated with the 3 mm thick CTE samples. Similar capsules to the one shown in Fig. 4a containing IG-430 graphite, but containing other grades such as POCO ZXF 5Q, SGL R7650 and Carbone made up the graphite irradiation volume upstream of the isotope targets. The proton energy in the IG-430 layers ranged between 155 and 145 MeV. Detailed analyses using advanced Monte Carlo based transport codes MARS-15 and FLUKA [41–43] concluded that energy degradation is not expected to have any significant impact on the induced irradiation damage across the 1 mm sample thickness based on the almost uniform through thickness energy deposition. Specifically, total beam energy degradation (dE/dx) across the 1 mm thick tensile samples was estimated to be ~1 MeV. In a latter section, experimental results on the through thickness variation of the lattice c-parameter in the proton-irradiated samples confirm the energy beam energy deposition through-thickness uniformity. Due to the 3-sample stacking – and thus the heat transfer through the stack and the capsule's 0.3048-mm thick 304 stainless steel windows (front and rear) to the heat sink (forced flow past outer face of window) – temperature differences of <10 °C (depending on the location on the plane) were estimated by the thermo-mechanical finite element analyses studies [44]. This difference in temperature is evident also in the c-parameter variation which is depicted in a later section (Fig. 12c).

The total flux of protons incident on the IG-430 graphite array was 3.3 10^{21} (integrated beam current ~144,310 µA-h) and the beam profile was characterized by σ_x ~6.6 mm σ_y ~7.0 mm. The 2-D Gaussian profile of the proton beam was deduced from radiographic analysis of a Ni foil inserted in the array. The foil radiographic analysis revealed a beam offset quantified as x_o ~4.0 mm (horizontal) and y_o ~2.0 mm (vertical). Should be noted that the beam offset was further confirmed from post-irradiation activity measurements of the type-B samples (Fig. 5b). Based on the integrated current of ~3.3 10^{21} protons, the Gaussian beam profile and the offset the fluence throughout the capsule was estimated. Average values were used for type-B (CTE samples) for dilatometer-based dimensional changes. The tensile (dog-bone) samples were characterized by the peak fluence estimated within the 6-mm gauge (central, narrow section). The peak fluence was estimated to be ~1.14 10^{21} p/cm^2. Fluence in the type-B samples used for dilatometer-based dimensional change along the 29 mm dimension

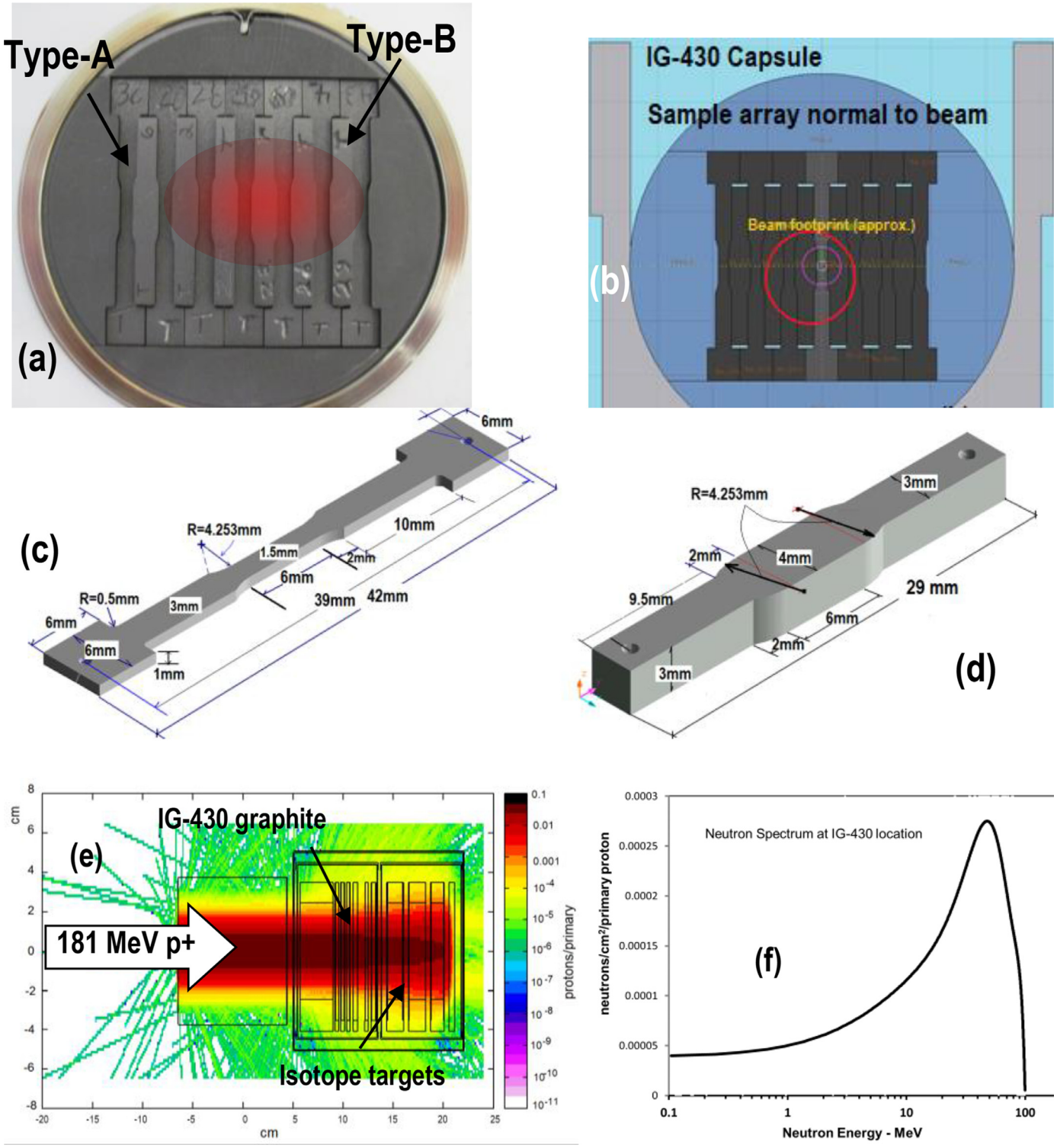

Fig. 4. (a) IG-430 graphite specimen layout and specimen geometry (type-A and type-B) used in the proton and spallation neutron irradiations (designation T on specimens stands for Toyo-Tanso), (b) replication of the sample array into the transport code used for proton beam degradation, energy deposition and damage assessment, (c) dimensions of type-A sample, (d) dimensions of type-B sample in the array, (e) proton-irradiation layout with graphite targets/capsules upstream of isotope producing targets, (f) neutron spectrum at the location of the IG-430 graphite capsule during neutron irradiation.

was averaged with peak at ~6.1 10^{20} p/cm^2. For growth and ultrasonic measurements of type-B samples the actual fluence rather than averaged at the midsection was used based on the position of the sample in the array. Energy deposition estimated by the transport codes [41–43] in the 3D volume of the entire array (peak power density ~ 395 W/g) was input into a benchmarked thermomechanical model [44] for irradiation temperature estimations. Due to the layout of the target station at the end of the 200 MeV Linac where irradiations were conducted (BLIP endstation) no direct sample irradiation temperature measurements are possible due to the hermetically sealed configuration. The adopted numerical models used, however, have been well benchmarked on

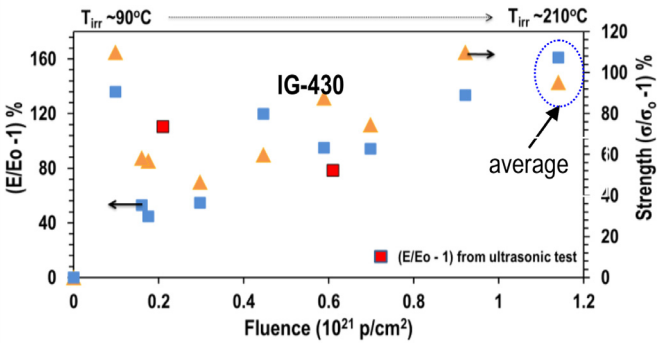

Fig. 5. Fractional change in Young's modulus and fracture strength following proton irradiation at irradiation temperatures 120–210 °C. Note: Maximum fluence values shown are averaged between three test samples.

experimental data over the years in support of irradiation experiments at the BLIP facility. This was done in order to eliminate uncertainties and ensure, primarily, uninterrupted medical isotope production that takes place in tandem with material irradiation studies with irradiation temperature estimation being one of the critical parameters**.**

In addition to the two proton irradiations reported herein, spallation fast neutrons generated from 118 MeV protons at the BLIP beamline were used to irradiate a capsule with IG-430 samples (similar to the one shown in Fig. 4a) also in argon atmosphere. The estimated irradiation temperature during fast neutron irradiation which reached a fluence of ~6 10^{19} n/cm^2 (>0.1 MeV) was T_{irr} ~80 °C with the neutron fluence approximately uniform over the IG-430 array. The fast neutron spectrum at the location of IG-430 irradiation is shown in Fig. 4f where the neutron flux was estimated to be ~8.6 × 10^{10} n/cm^2/s, the γ flux 1.3 × 10^{11} γ/cm^2/s and the electron flux 2.85 × 10^9 e/cm^2/s. The importance of the γ flux during neutron irradiation and its role in annealing during irradiation has been discussed in [8].

Primary objective of the fast neutron irradiation was to achieve comparable fluence (and irradiation temperature) between samples in the extreme locations of the proton irradiation campaign and the spallation neutrons, albeit moderate fluences. This would enable the establishment of a reliable correlation between damage from protons and fast neutrons through the post-irradiation analyses.

3. Post-irradiation analyses

One of the objectives is to test how IG-430 graphite irradiated with higher energy protons adheres to similar damage behavior observed and reported in several studies focusing on reactor neutrons. To achieve that a comprehensive, multi-faceted PIE was launched to assess changes in mechanical properties, thermal properties (including dimensional changes and growth, thermal expansion), stored energy release potential in this grade, and finally crystallographic changes. Any comparison, however, should be made with caution even if the irradiation experiments using protons and neutrons reached similar fluences and conducted at similar irradiation temperatures. This cautionary note stems from the fact that neutron interaction with matter results in ballistic collisions, while energetic proton interactions are ionizing with essentially no ballistic collisions.

3.1. Mechanical properties and post-irradiation annealing effects

The effect of proton irradiation and subsequent post-irradiation annealing on the tensile strength and Young's modulus of graphite was studied by (a) conducting tensile tests on irradiated samples (some of which were annealed prior to the mechanical test) and (b) by correlating the change in the ultrasonic velocity, as a result of micro-structure damage, to the elasticity modulus including the effects of post-irradiation annealing. Fig. 5 depicts the increase in Young's modulus and strength as a function of proton fluence in the IG-430 graphite as deduced from mechanical tests performed on type-A (1 mm thick tensile specimens). Added in Fig. 5 are changes in Young's modulus for the IG-430 graphite deduced from ultrasonic tests on the type-B specimens of the irradiated array shown in Fig. 4a and b. These irradiated IG-430 samples are 3 mm thick (instead of the 1 mm thickness of the tensile samples in the capsule). Two type-B samples that had not undergone post-irradiation thermal annealing are plotted in Fig. 5. Fractional change (E/Eo-1) in graphite irradiated with neutrons have been published in [26] for three different temperature regimes, 160–179 °C, 200–219 °C and 240–259 °C. It was observed in [26] that the fractional changes of both Young's Modulus and strength to undergo rapid saturation particularly at the lower irradiation temperature and pass through a maximum before saturating. It was concluded [26] based on their data that changes in moduli and strength are extremely insensitive both to the quantity and quality of the damage.

A 5 kN Tenius-Olsen mechanical testing machine operating at 1 mm/min setting was used for the mechanical tests of graphite. Particularly, a special fixture was designed to enhance both the gripping of the graphite tensile samples (see Fig. 4c) and preventing any misalignment during pulling of the relatively fragile graphite samples. No strain gauges were used within the 6-mm gauge portion of the tensile sample due to the radiation safety concerns (elevated dose and activation from 8-week bombardment with intense proton beams) and the experimental set-up itself (remote testing within the hot cell). Machine compliance was not believed to be an issue at these load levels. Tensile tests were conducted at room temperature.

The stress-strain behavior of unirradiated IG-430 graphite is shown in Fig. 6a which reveals limited data scattering from sample to sample and an average tensile strength of 37.5 MPa which confirms the Toyo-Tanso company listed value of 37.8 MPa [39]. Fig. 6b depicts the evolution of strength and Youngs modulus with proton fluence and post irradiation annealing. As seen in Fig. 6b the reduction in Young's modulus is accompanied with significant reduction in irradiated strength of IG-430. The reduction in E and strength with increased dose (Fig. 6b) is attributed, in part, to the increasing basal plane separation distance that takes place [20] and primarily to the Wigner energy release and the point defect recovery. During irradiation individual graphite crystals undergoing irradiation growth grow into and fill the pores introduced during manufacturing. The observed increase of the elastic modulus is assessed to not be the result of dislocation pinning due to the fine-grain nature of IG-430 graphite but rather the result of cross linking of graphite planes [10]. Important to note in Fig. 6b is the effect of post-irradiation annealing which tends to reduce both the gained strength and the increased by irradiation Young's modulus, an effect attributed to irradiation induced creep [33]. The test samples of 0.6 and 1.14 1021 p/cm^2 fluence shown in Fig. 6b that were heat treated following irradiation and prior to mechanical testing were annealed to 220 °C, dwelled for 1.5 h, heated to 300 °C where they dwelled for 1 h. The heating rate between room temperature and 220 °C and between 220 and 300 °C was 2 °C/min.

Ultrasound-based experiments conducted on the 3 mm thick samples (type-B), which also explored included the effect of post-irradiation annealing are shown in Fig. 6c. The tests were conducted using a Panametrics EPOCH-4 system and dual ultrasonic transducer of 2.25 MHz frequency on the 3 mm thick type-B or CTE specimens. By relating the changes of the ultrasonic velocity through the material with the changes in Young's modulus,

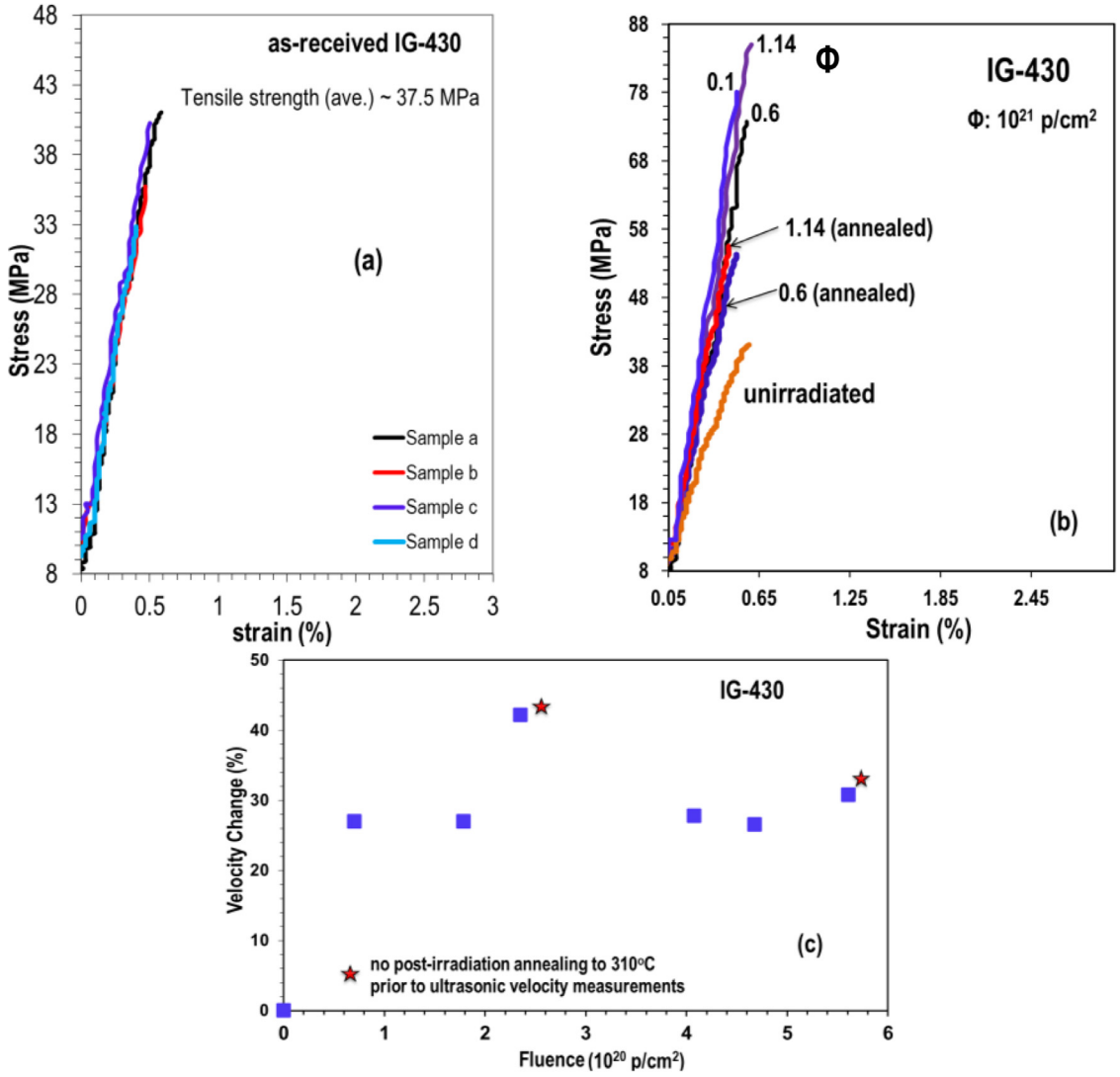

Fig. 6. (a) Stress–strain behavior of as-received (unirradiated) IG-430 graphite, (b) effects of proton irradiation and post-irradiation annealing on stress-strain behavior of IG-430, (c) ultrasonic velocity changes in proton-irradiated IG-430 as a function of proton fluence and post-irradiation annealing.

the effect of irradiation dose and subsequent annealing is established. The relationship may be used to relate the measured longitudinal velocity υ with the Young's modulus E (for constant density ρ and Poisson's ratio η) resulting in percentage increase in the modulus E estimation. These results confirm the findings of the mechanical tensile tests (i.e. partial recovery of Young's modulus with post-irradiation annealing) and are in line with previous observations [18, Burkholtz] where the Young's modulus increases with fluence, reaches a maximum and begins a downward trend with increasing fluence, as can be seen from the untreated samples (with asterisk). Based on results presented in [18] Young's modulus of graphite irradiated with neutrons at room temperature increase by approximately a factor of three up to 1020 n/cm^2 and starts to decrease at higher fluences. Such changes in Young's modulus and strength were observed to be smaller at higher irradiation temperatures, a trend that can also be seen in the present study for IG-430 under proton irradiation (Fig. 6b).

3.2. Dimensional changes and growth

Irradiation of graphite with energetic protons is expected to result in dimensional changes of considerable magnitude. The behavior of graphite lattice under irradiation is characterized by growth perpendicular and shrinkage parallel to the basal planes. For the aggregate, and in particular for isotropic graphite such as IG-430, the overall effects or global dimensional changes along the normal or parallel directions cannot be distinguished. Porosity introduced during manufacturing of the graphite will be reduced as graphite crystals experience irradiation-induced growth and grow into the pre-existing pores. Therefore, and following irradiation, evidence of porosity reduction will be partially revealed by the trace of the linear expansion with temperature increase. Prior to the linear expansion in post-irradiation, the graphite structure would experience growth or shrinkage depending on both the dose and the irradiation temperature, which in addition to pre-existing porosity evolution, is driven by the growth or shrinkage of individual crystallites. In this study, measurements of proton irradiation-induced overall dimensional change were made for IG-430 and were compared to measurements made on the isotropic graphite POCO ZXF 5Q irradiated under similar conditions. As seen in Fig. 7a, IG-430 samples irradiated at temperatures ~180–200 °C experience growth that displays a downward trend with increasing dose, a trend that is in general agreement with neutron data shown in Fig. 7b [27] from studies at Brookhaven Graphite Research Reactor (BGRR).

Dimensional changes and annealing of irradiated IG-430 in this study were measured using a high-precision LINSEIS dilatometer

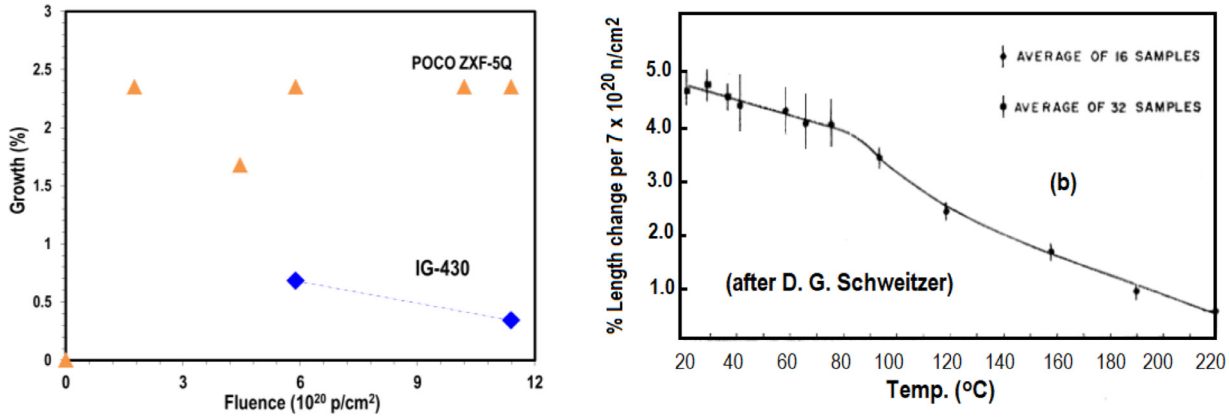

Fig. 7. (a) IG-430 proton irradiation-induced growth in the temperature range 180–200 °C with comparison to POCE ZXF 5Q graphite, (b) rates of growth from neutron irradiation in 20–220 °C range.

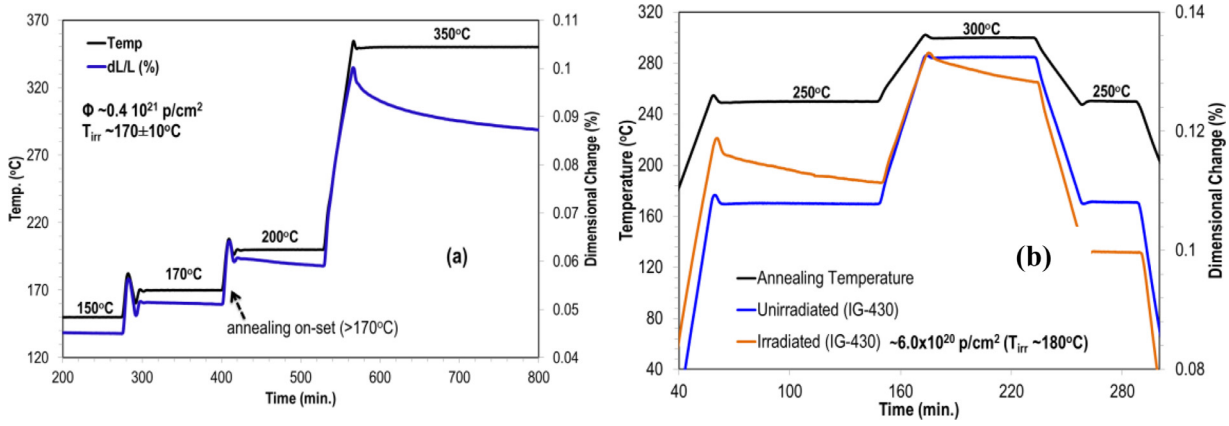

Fig. 8. (a) Annealing of IG-430 following proton irradiation at T_{irr} ~170 °C and identification of damage reversal triggering temperature, (b) annealing of IG-430 following proton irradiation at ~180 °C with isotherms at 250 °C, 300 °C and again at 250 °C revealing damage annealing characteristics.

(dual rod, horizontal). During post-irradiation annealing the thermal expansion is expected to be linear up to the irradiation temperature stemming from the fact that annealing of radiation-induced defects is taking place concurrently with irradiation. During irradiation, interstitials accumulate between basal planes resulting in an overall volumetric growth of the polycrystalline structure. The contraction that is taking place above the irradiation temperature stems from activation of interstitials that are further away from the lattice planes and require higher activation energy for mobilization (return to unoccupied positions or vacancies on the lattice plane). Fig. 8(a, b) depict the post-irradiation annealing behavior of a sample whose position is indicated in the test array relative to the proton beam (T designation indicates Toyo-Tanso or IG-430). The heating rate during the experiments was 2 °C/min and the hold time varied (indicated on the axis in minutes). As seen in Fig. 8 and up to 170 °C isotherms, there is no dimensional change under constant temperature indicating that annealing of interstitials has taken place during irradiation. Only at higher temperature isotherms one observes contraction of the irradiated IG-430 sample stemming from temperature-induced interstitial atom migration back to the basal planes. This is further confirmed in Fig. 8b where upon return to an isotherm (250 °C) above the irradiation temperature (<200 °C) from an even higher temperature (300 °C) the IG-430 structure/lattice experiences no contraction since all the interstitials that could be mobilized at this temperature have already returned to vacant lattice positions.

Shown in Fig. 9a is thermally-induced annealing at higher temperatures in irradiated IG-430 showing that with each additional annealing cycle there is diminishing net dimensional change as a result of interstitial mobilization and annealing. Fig. 9b depicts the post-irradiation annealing behavior of IG-430 irradiated to different combination of fluence/temperature at temperatures up to 540 °C revealing that upon thermal annealing most of the induced damage has been reversed resulting in a stable structure.

Wigner or stored energy in graphite moderators resulting from the damage of the graphite crystal lattice is a matter of great importance. The characteristics of energy release are expected to vary depending on the dose, flux, and irradiation temperature. A great deal of work has been done in this field in an effort to gain understanding of this energy release. Several nuclear graphites [20,26,27] were shown to exhibit a change in the rate of dimensional expansion with neutron irradiation after exposures of ~ 6 10^{20} at 30 °C. In [26] stored energy and dimensional changes in reactor graphite were investigated following irradiation by fast neutrons for a range of temperatures (30 °C–300 °C) and irradiation doses to 10^{21} n/cm^2. Changes in crystal lattice parameters and the associated dimensional changes in the polycrystalline reactor graphite and their correlation with growth have been presented in [26,27]. While annealing experiments and measurements of stored energy removal [26,27], including the present study, identified specific temperatures at which stored energy release occurs, theories vary as to the actual process behind it. Theories agree that Wigner energy is stored in the defect structure of graphite caused by neutron irradiation (i.e. interstitial atoms, vacancies, and other aggregate defects which raise the internal energy) but they differ on the process causing its release, either by defects attaining a stable

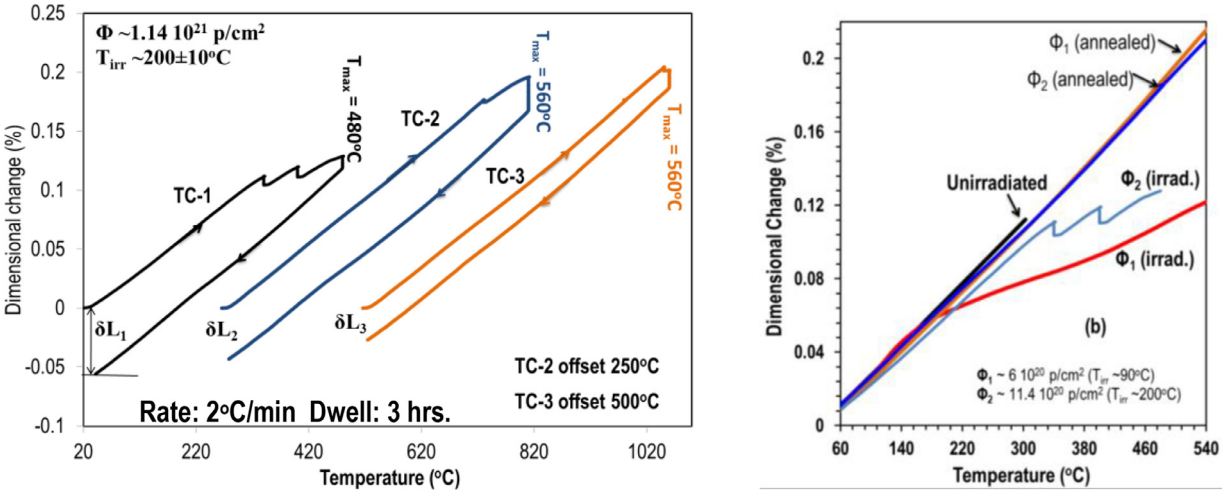

Fig. 9. Multi-thermal cycle thermal annealing of IG-430 characterized by isotherms up to T_{max} =560 °C (heating rate 2 °C/min and hold times of 3 h) following proton irradiation at ~200 °C. Evolution of dimensional recovery (δL) with annealing. Note: SUM of δLs will produce the total reclaimed dimensional change due to irradiation.

configurations at a lower energy level (thus releasing excess energy in the process) or through interstitial-vacancy recombination.

First principle calculation have been performed [28] addressing the recombination of vacancies and interstitials on the basal plane of graphite searching for activation energy mechanisms and thresholds concluding that the most favorable process in-plane is vacancy diffusion associated with an activation energy which is lower than that of the interstitial and the direct-exchange mechanisms between interstitial and vacancies. A different atomic processes associated with energy storage and release is argued in [29] where the production of interstitial and vacancy pairs and their recombination which releases energy in the process is postulated to be the cause of Wigner energy release peak in graphite at around 200 °C. Also argued in [10] is that the observed energy release stems largely from the combination of Frenkel pair annihilation, graphite layer nano-buckling removal and point defect migration and aggregation.

It was pointed out [26,27], however, that no direct experimental evidence actually exists which can distinguish whether the observed effect (the 200 °C stored energy release) is due to a change in the apparent volume of the defects produced by irradiation or whether a change in the rate of accumulation of defects occurs after large exposures. The above cited studies have considered the effects of neutrons on graphite structures. In the present study we evaluate stored energy release from this fine-grained IG-430 irradiated with energetic protons at temperatures below the 200 °C threshold. Shown in Fig. 10 is the stored energy release for irradiated IG-430 at low temperatures (~90–140 °C). Stored energy release is studied by tracing dimensional changes during the first post-irradiation annealing cycle (TC-1). In [30] ion and electron irradiation effects on carbon nano-tubes and nano-systems were reviewed and compared to graphite (particularly the relationship between point defects in the nano-systems and graphite) with focus on defect migration in graphite, carbon interstitials and bonding with lattice atoms. Discrepancies were noted in migration energies due to interpretation of experimental observations. Specifically, the review [30] concluded that it is still not clear which particular type of defects can be associated with annealing peaks observed during annealing experiments (similar to the ones observed for IG-430 in the present study shown in Fig. 10a).

In normal dimensional change behavior of irradiated graphite (no energy release) shrinking is observed as a result of interstitial atom annealing leading to trace that deviates from the baseline (unirradiated) below the baseline trace. Upon further annealing cycles the irradiated material approaches the baseline as seen in Fig. 10a for the trace of Φ_2 ~10^{20} p/cm^2 and T_{irr} ~110 °C. During stored energy release (as observed in Fig. 10a for Φ_1 ~4 10^{20} p/cm^2 and T_{irr} ~140 °C) an increase in the rate of dimensional change is observed that is practically over at ~200 °C. These observations for graphite irradiated with protons at these low temperatures (T_{irr} 90 °C and 140 °C) tends to be contrary to the conclusions reached by other studies [7,9] where thermal expansion of graphite without stored energy (for T_{irr}>300 C) is greater than for unirradiated graphite for low to intermediate fluences and lower at high fluences. Should be noted that for this higher dose, **Φ_1**, the gradual increase is also accompanied with a very abrupt change or a spike. Such behavior (i.e. presence of a spike) has been shown to occur in only some of the graphite samples of the irradiated array tested (similar but not exact irradiation conditions of fluence and temperature) and exhibited energy release. It appears as though a very precise combination of irradiation temperature and fluence is responsible for stored energy to be released or not. What is also confirmed in Fig. 10a is that, whether the IG-430 test sample has released stored energy or not, upon subsequent thermal annealing the tendency to approach the unirradiated material through damage annealing is similar, a response that is typical in stored energy removal.

Irradiation-induced changes in the coefficient of thermal expansion (CTE) in polycrystalline graphite are quite complex [14–16] and not well understood, particularly at low irradiation temperatures. The effect of irradiation on the CTE is strongly dependent on material history, direction of cut and irradiation temperature [22]. At room temperature, the coefficient of thermal expansion increases with dose until, at ~5 10^{20} *nvt*, beyond which it begins to decrease. The irradiations of IG-430 graphite in the present study were conducted at higher than room temperature (90–210 °C). Shown in Fig. 11a is the CTE of IG-430 at 250 °C as a function of proton fluence. A trend is also observed where, as in neutron irradiated graphite reported in [22], of decreasing CTE above the fluence threshold of ~5 10^{20} *nvt*. For comparison purposes the CTE at 250 °C of the IG-43 graphite (unpurified version of IG-430) [39] for low proton fluence irradiation is shown in Fig. 11b while at Fig. 11c the change of CTE of IG-430 and IG-43 graphite grades irradiated at ~90 °C to ~10^{21} p/cm^2 is shown as a function of temperature. The IG-43 grade is created through cold isostatic pressing (CIP), it is isotropic with density of 1.82 g/cm^3 and exhibits a tensile strength of ~37 MPa (both properties similar to IG-430). The supplier's (Toyo-Tanso [40])

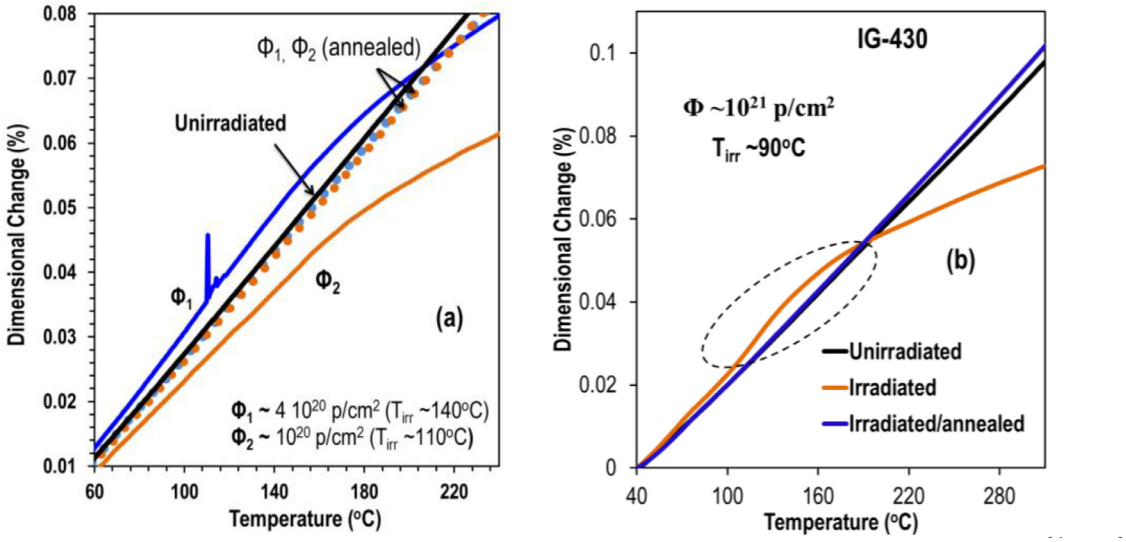

Fig. 10. Post-irradiation heating of G-430 following 200-MeV proton irradiation to ~10^{21} cm^2 at T_{irr} ~90 °C revealing damage reversal upon annealing and the release of stored energy in IG-430 only. (c) Stored energy release in IG-430 irradiated with 160 MeV protons at T_{irr} ~140 °C while no energy release is seen for lower irradiation temperature and fluence.

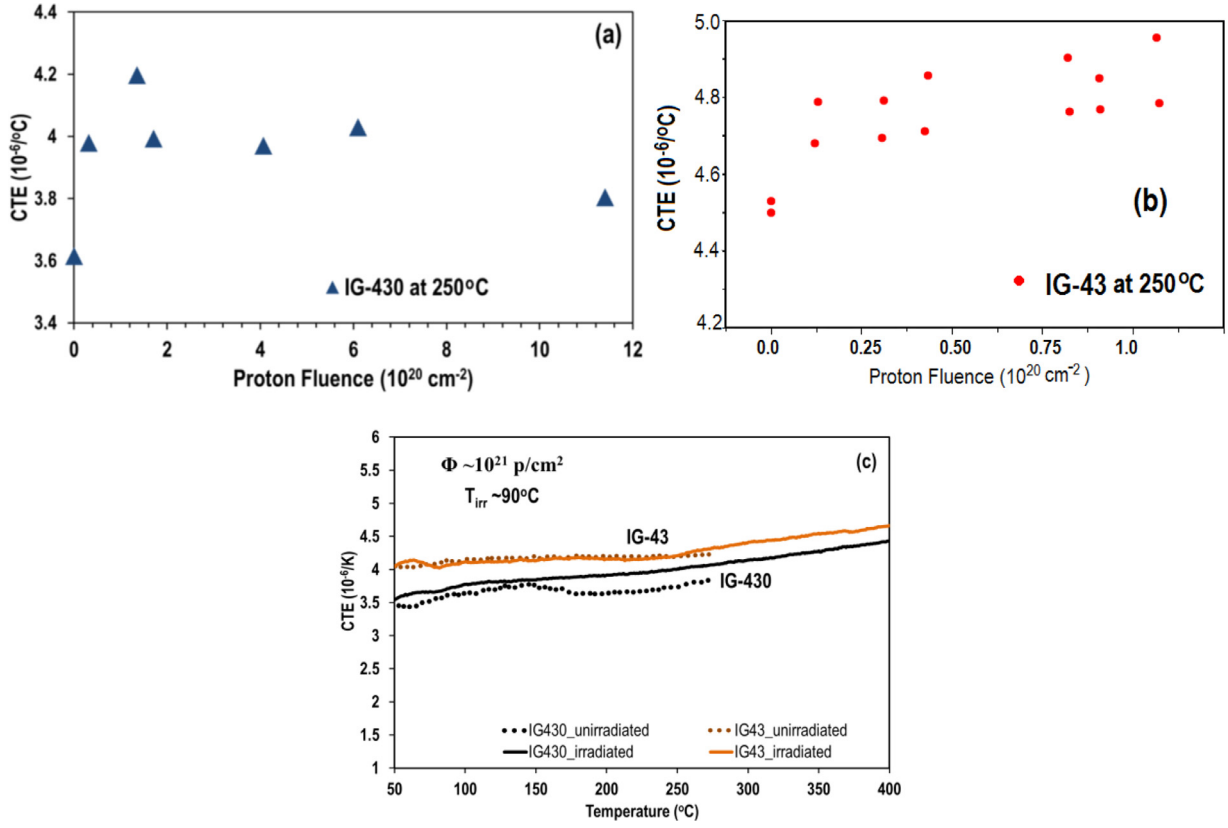

Fig. 11. Thermal expansion coefficient at 250 °C of (a) IG-430 and (b) IG43 as a function of proton fluence. (c) Evolution of CTE with temperature of irradiated IG-430 and IG43.

average CTE for unirradiated IG-430 in the temperature range 350–450 °C is 4.8 × 10^{-6}/°C. CTE results of the present study shown in Fig. 11 that appear slightly lower are not average values. The low-fluence peak (Fig. 11a) of the IG-430 is attributed to the closure of the Mrozowski cracks that accommodate the initial densification, which according to [6] are not as extensive as in the IG-110 grade. This explains the less distinguished peak in the low dose regime as compared to the more pronounced peak reported in [7] for the fine-grain nuclear graphite grade G347A from Tokai Carbon Co. Ltd.

3.3. X-ray diffraction

Proton-induced damage on the microstructure of IG-430 was studied using X-ray diffraction (a) of 200 keV polychromatic X-rays coupled with EDXRD technique where diffraction patterns from a small interaction volume within the bulk of the graphite sample (40 across the 1mm thick sample) where collected and (b) diffraction patterns in a transmission mode were collected using a 67 keV monochromatic mode and XRD technique.

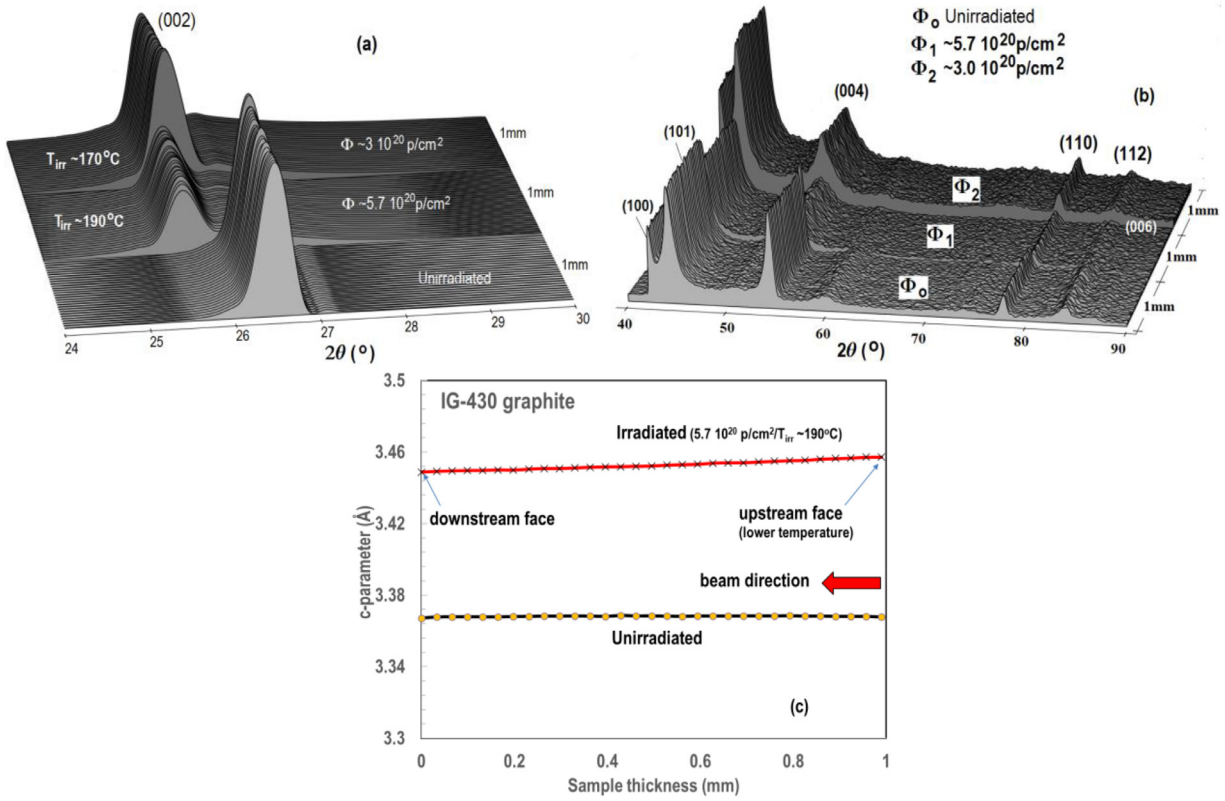

Fig. 12. 3D phase map of irradiated IG-430 compared to as received material. (a) Basal plane reflection, (b) in-plane and other reflections. Displacements-per-atom corresponding to the two fluences were calculated to be 0.11 and 0.056 DPA for $\mathbf{\Phi_1}$ and $\mathbf{\Phi_2}$ respectively. (c) Variation of c-parameter across the 1 mm thick sample for unirradiated and irradiated (upstream face where beam enters and downstream face where it exits) samples.

Shown in Fig. 12 are diffraction patterns across the 1mm thickness of unirradiated (baseline) and two irradiated samples of fluence $\mathbf{\Phi_1}$ ~5.7 10^{20} p/cm^2 (estimated equivalent of 0.11 displacements-per-atom, DPA) and $\mathbf{\Phi_2}$ ~3 10^{20} p/cm^2 (0.056 DPA). Fig. 12a depicts the effect of proton damage on the (002) reflection (basal plane) across the thickness indicating uniformity of damage across the 1 mm thickness of the sample. The corresponding c-parameter change for $\mathbf{\Phi_1}$ (~5.7 10^{20} p/cm^2) deduced from the tests is 2.83% and for the lower fluence $\mathbf{\Phi_2}$ (~3 10^{20} p/cm^2) is 2.536%.

With the applied EDXRD technique forty (40) reflections across the 1mm sample thickness (from the front face of the sample to the rear) were collected from gauge volumes within the bulk of the sample. This allows for the observation of **c**-parameter change across the thickness of the graphite sample that would result from through-thickness temperature variation and changing beam energy. Changing irradiation conditions within the thickness would also result in peak height variation. As noted in Fig. 12a there exists uniformity of both height and diffraction angle 2θ shift indicating that the variation is insignificant. Similar effects are seen in Fig. 12b which also reveals the disappearance of (006) reflection with irradiation. The degree of shifting and broadening of the (002) reflection with irradiation is more clearly shown in Fig. 13a where added for reference is the reflection following spallation neutron irradiation at ~80 °C and achieved fluence approximately an order of magnitude lower. Shown in Fig. 12c is the variation in lattice c-parameter resulting from the temperature variation (<10 °C) across the thickness of the irradiated 1 mm thick tensile sample. As previously noted, the beam energy deposition does not vary as the beam traverses the 1 mm graphite sample, but the resulting temperature experiences a small gradient due to the configuration of the 3-stack sample and the resulting heat transfer to the heat sink outside the capsule. The EDXRD technique allowed for several diffraction measurements within the 1 mm sample thickness (marks on traces indicate measurements). As shown in Fig. 12c, no variation is seen, as anticipated, in the unirradiated sample. The irradiated sample on the other hand (whose upstream face is in contact with the inside face of the cooled capsule entrance window) exhibits a gradient with higher c-parameter values on the lower temperature side.

On Fig. 13b the damage on the basal plane observed through the evolution of the (110) peak indicating shrinkage of the basal plane with irradiation is depicted. In [25] where samples were irradiated at a temperature of ~325 K with an average fast neutron flux of 2 × 10^{12} n/cm^2-s it was determined that even at low irradiation doses dislocation-mediated amorphization process takes place in graphite.

Shown in Fig. 14 are 200 keV polychromatic X-ray diffraction results (EDXRD) and comparison between IG-430 grade and its un-purified predecessor IG-43 irradiated at similar proton fluences (~10^{21} cm^{-2}) and low temperatures (210 °C for IG-430 and ~90 °C for IG-43). Caution must be exercised in the direct comparison of the two grades due to the irradiation temperature differences. While both irradiations were conducted below the temperature threshold (200–250 °C) which has been observed to distinctly separate stored energy release and crystal structure evolution [10,20,22,27], irradiation temperature, variation even within the low temperature regime, can have a significant impact on the graphite crystal expansion [20]. Observed in Fig. 14 is the diffused form of the basal reflection (002) of the irradiated IG-43 indicating fragmentation of the crystallites into smaller grains.

To further understand or confirm the high degree of diffused form (002) reflection observed in IG-43 which is supposed to only differ from IG-430 in that it has not undergone purification, we compared it to POCO ZXF 5Q graphite which was

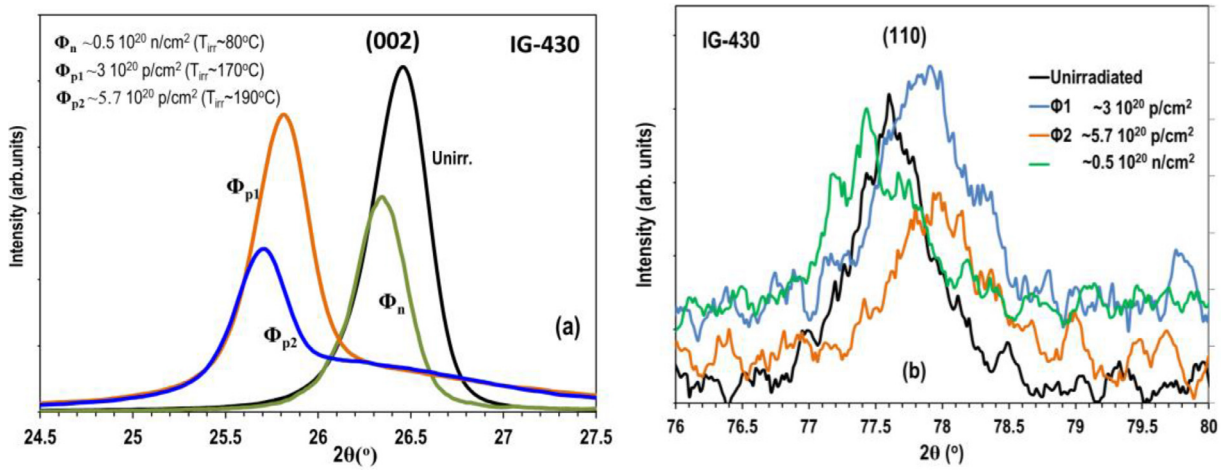

Fig. 13. (a) Effect of proton and lower dose fast neutron irradiation on (002) reflection, (b) dose effects on (110) reflection.

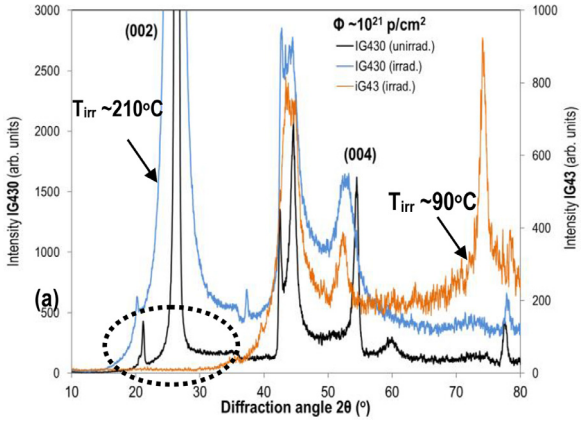

Fig. 14. Proton irradiation effects on the crystal structures of IG-430 and IG-43 irradiated at 210 °C and 90 °C, respectively, using 200 keV polychromatic X-rays and EDXRD technique comparing the evolution on the basis of similar fluence received within at two different low-temperatures.

irradiated with very energetic protons (120 GeV) to a high fluence ~8.6 10^{21} p/cm^2. X-ray diffraction results [13] had shown similar diffused (002) reflection to IG-43 that was subjected to approximately eight times lower fluence but at lower irradiation temperature. Shown in Fig. 15 shows the evolution of the (002) and (110) reflections in IG-43 (a, b) as a function of increased proton fluence (and irradiation temperature) contrasted with changes observed in POCO ZXF 5Q (c, d). Insert TEM images in Fig. 15c and d show the condition of the graphite structure [13]. Interesting to note is the jagged trace of the (110) reflections of IG-43 as fluence increases towards 1.1 10^{21} p/cm^2. Also noticed is the fact that while the basal plane reflection (Fig. 15a) diffuses monotonically (i.e. with increasing fluence), that is not what is observed with the in-plane (110) reflection. As shown in Fig. 15c and d, much higher fluence levels than those experienced by IG-43 were required in the POCO ZXF 5Q graphite grade [13] to result in the diffuse state observed and depicted in the TEM image. In assessing the IG-43 response to these lower irradiation fluences, it is only the opinion of authors that the tendency of the IG-43 graphite to exhibit the diffuse state (disappearance of the basal reflection) to be partly attributed to the lack of purification in this grade as compared to its purified IG-430 counterpart. Further studies are required to understand or prove that purification is indeed a contributing factor.

XRD with 67 keV mono-chromatic beams: Utilizing the brilliant 67 keV X-rays at the XPD beamline of the NSLS II a comprehensive analysis of the proton irradiated IG-430 grade was conducted focusing on the confluence of irradiation dose and temperature on the crystal structure changes. Specifically, an array of IG-430 test samples spanning irradiation temperatures between 90 and 210 °C and fluences in the range of ~0.08–1.2 10^{21} p/cm^2 underwent X-ray diffraction in transmission mode of the 500 × 500 μm beam profile. Fig. 16 depicts the 2D detector image comparison between the proton irradiated and as received IG-430 state revealing the broadening effects on the (002) reflection.

It has been observed and reported in several studies of neutron irradiated nuclear graphite [19,22,20,29] that the (002) reflection at low irradiation temperatures undergoes a significant evolution characterized by strong, asymmetrical broadening above the critical fluence of ~5 10^{20} n/cm^2 while a strong influence of the irradiation temperature on the lattice parameter expansion is observed leading up to the fluence threshold. Beyond the critical fluence strong broadening of the (002) X-ray line has been observed indicating that periodicity of the lattice is heavily disturbed. Fig. 17a presents the effects of proton irradiation on the evolution of the (002) reflection as a function of irradiation temperature (a1 and a2 depict data on the two sides of 150 °C respectively) and fluence clearly demonstrating similar behavior to that reported on nuclear graphite under neutron irradiation. In general agreement with observations made under neutron irradiation [31] – where a transition fluence of ~6 10^{20} n/cm^2 (low vs. high dose) was identified where broadening of the (002) reflection becomes important while up to ~4 10^{20} n/cm^2 the lattice expands in the c-direction linearly – IG-430 and for fluence above 5–6 10^{20} p/cm^2 also undergoes significant broadening and enters turbostratic state (breaking of crystals into smaller crystallites). Fig. 13a deduced using EDXRD with 200 keV polychromatic beam demonstrates similar transition. Fig. 17b (b1 and b2) depicts the evolution of the (110) reflection. The evolution of the (112) reflection for the two fluence/temperature ranges is depicted in Fig. 17c indicating that the anticipated reduction of the peak with increased dose is not accompanied with any shift in position as seen for the (002) and (110) reflections.

The percent change in the c- and α-parameters of IG-430 graphite as a function of proton fluence irradiated in the temperature range of 90–210 °C is shown in Fig. 18. Similar to what has been observed for nuclear graphite irradiated with fast neutrons at different temperatures [19,20], changes in the c-parameter are greater at the lower temperature regime.

Experiments using the 67 keV monochromatic X-rays and XRD on proton-irradiated IG-430 graphite enabled the study of the low end of fluence (~7 10^{19} p/cm^2) which is comparable

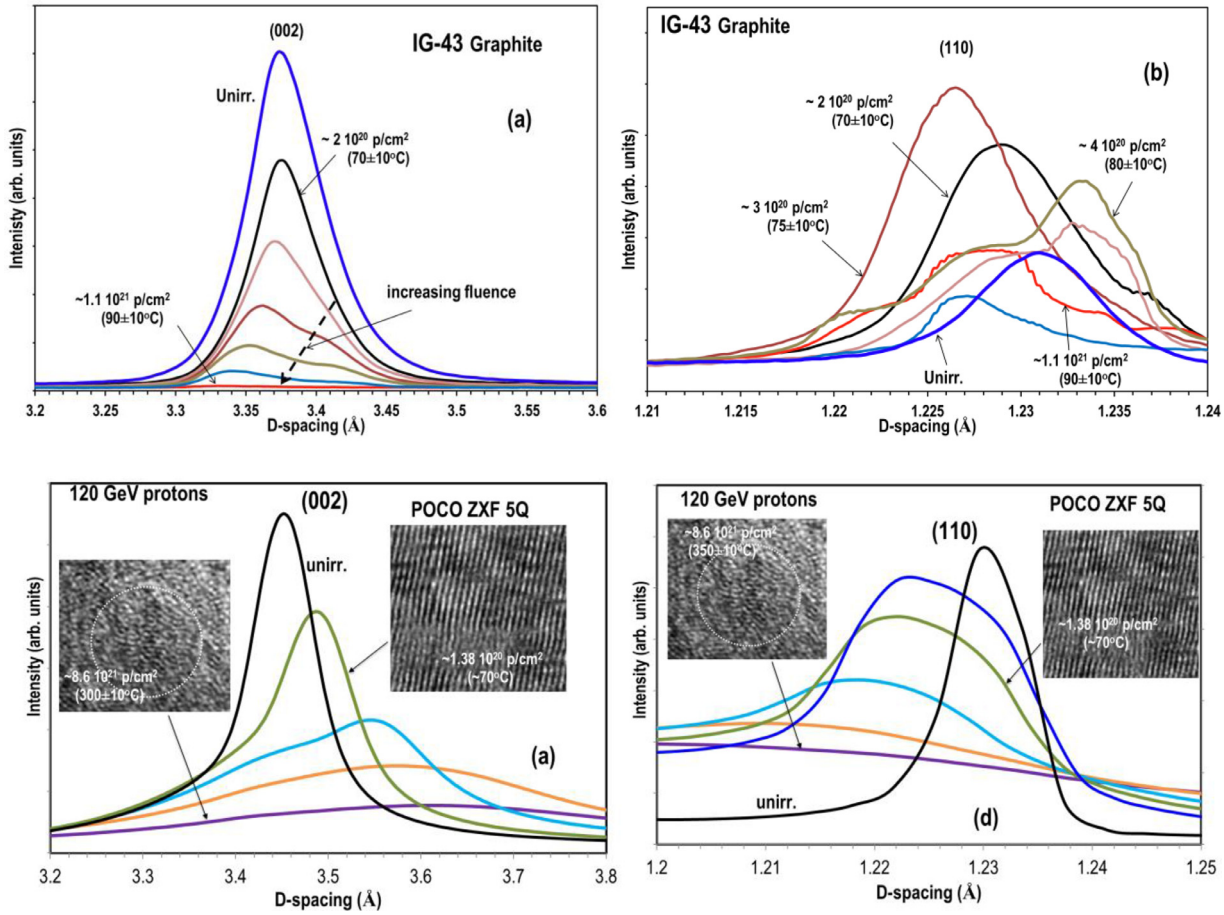

Fig. 15. Proton irradiation amorphization of the crystal structures of IG-43 and POCO ZXF 5Q irradiated by 120 GeV protons to 8.6 10^{21} p/cm^2. (a, b) 002 and 110 reflection evolution in IG-43, (c, d) 002 and 110 reflection evolution in POCO ZXF 5Q [13].

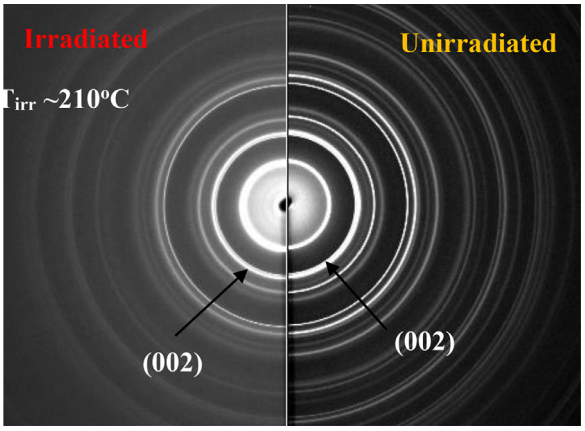

Fig. 16. 2D detector diffraction image of irradiated IG-430 to ~10^{21} p/cm^2 (left) at T_{irr} ~210 °C and unirradiated (right).

with the spallation neutron fluence achieved with spallation neutron irradiation (spallation neutron damage only evaluated thus far using EDXRD technique with 200 keV polychromatic X-rays, Fig. 13a). Specifically, irradiation with spallation (fast) neutrons to ~5 10^{19} n/cm^2 has resulted in a d_{002} of ~3.3850 Å, a change from d_{002} = 3.3681 Å for the unirradiated state. Comparable proton fluence (~7 10^{19} p/cm^2) and irradiation temperature (~90 °C) has resulted in a larger d_{002} of ~3.40 Å. The difference is attributed by the authors partially on the annealing effect of γ-rays that are produced during the spallation process with estimated flux 1.3 × 10^{11} γ/cm^2/s. Gamma-ray annealing in-reactor irradiations has been postulated in other studies [8] to effectively reduce damage from neutron. Other contributing factor could be that protons, due to their higher impinging energy (160 MeV), induce, for the same fluence as neutrons, higher damage in the graphite lattice.

4. Summary

Several irradiation campaigns with energetic protons of energies in the range of 120–200 MeV – including an irradiation campaign with spallation generated fast neutrons – were conducted at the BNL BLIP on IG-430 graphite under consideration for pion producing proton beam targets in particle accelerator initiatives such as the Neutrino Factory and the Long Baseline Neutrino Facility experiment. The experiments were conducted at relatively low temperatures (90–210 °C) with peak fluence achieved ~10^{21} cm^{-2} for protons and ~0.6 10^{20} n/cm^2 (> 0.1 MeV) for neutrons. Macroscopic and microscopic post irradiation analyses were performed on the irradiated IG-430 graphite with the latter relying on high energy X-ray diffraction at the BNL synchrotrons. Multi-faceted post-irradiation examination results were used to assess the evolution of macroscopic properties (strength, Young's modulus, growth and thermal expansion) as well as IG-430 graphite lattice changes under proton irradiation over the low temperature regime (90–210 °C), compare these effects and changes with those imparted by neutrons on similar nuclear graphites and identify any similarities in the trends and changes prompted by the two irradiating species. It should be emphasized that the current study which was

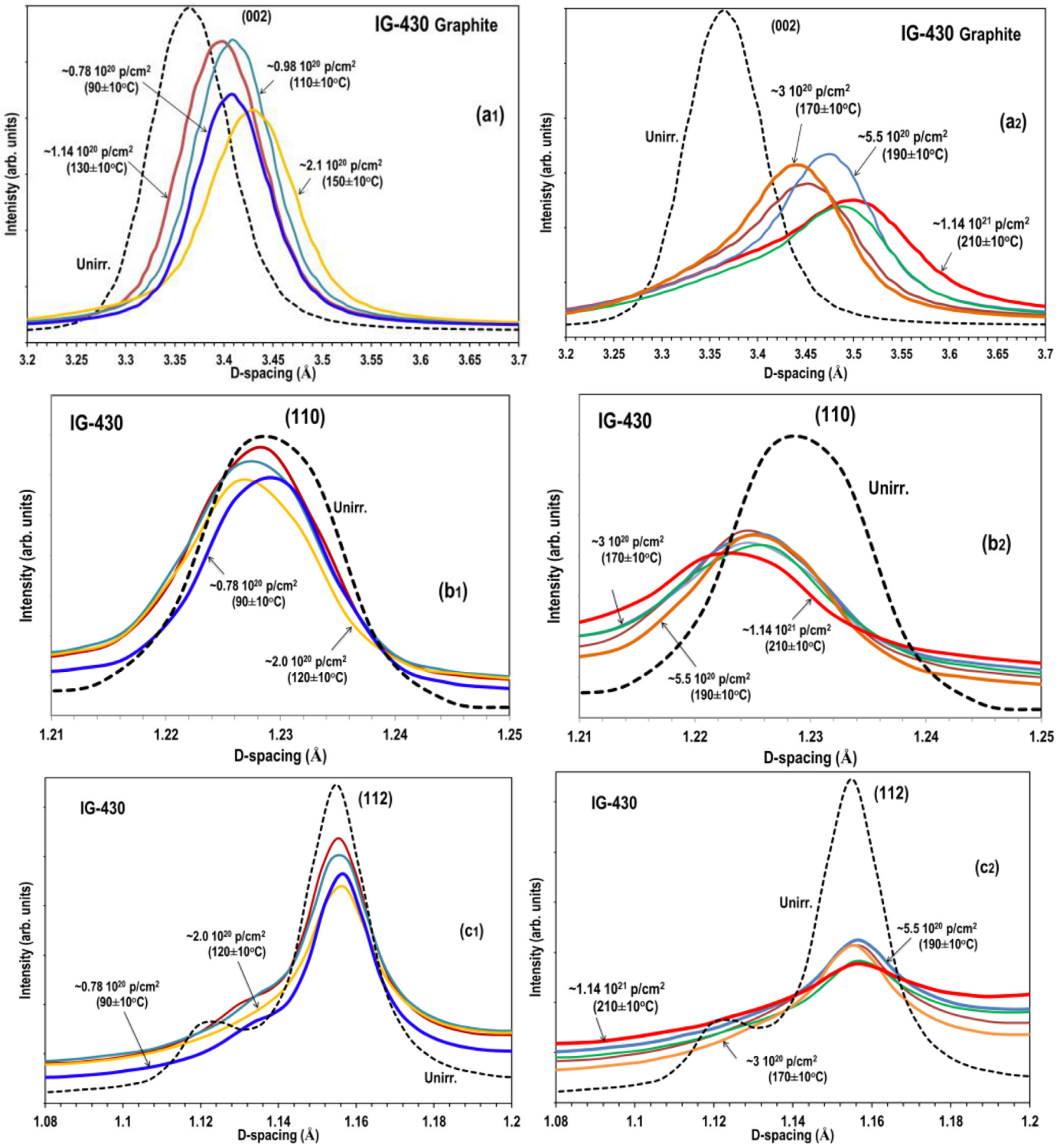

Fig. 17. Proton fluence and temperature effects on (a) basal, (b) plane and (c) 112 reflections of IG-430 graphite.

prompted and undertaken to serve an entirely different field (i.e., generation of neutrino beams) rather than nuclear reactor materials such as future Very High Temperature Reactors (VHTR), only aims to provide experimental information on one of the candidate materials with limited experimental data base to-date, IG-430 graphite, over the low temperature regime (<250 °C) which is inherently linked with more damage and physio-mechanical changes in graphite structures. Understanding low-temperature behavior of the candidate graphite even for VHTR is important, even if the behavior is deduced from an irradiating species other than fast neutrons, energetic protons in this case. Proton and other ion irradiations, a topic that has been the subject of several studies [8,34,37], may be valuable tools in aiding the understanding of in-reactor behavior of metals in general and graphite in particular. This study, taking advantage of energetic proton irradiation experiments conducted on the IG-430 graphite grade, a grade also a candidate in future reactor applications, explored and deduced irradiation-induced changes of its properties in the low temperature regime

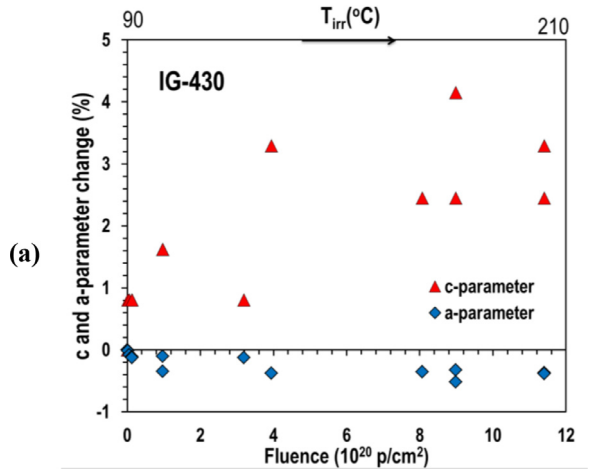

Fig. 18. Percent change in c- and a-parameter with fluence (temperature varies in displayed points between 90 and 210±10 °C).

that may provide some understanding of its behavior and aid, with further investigations, its candidacy as a reactor grade material.

This proton irradiation study has revealed the following:

- IG-430 graphite shows better graphitization than similar isotropic graphites (POCO ZXF 5Q, SGL).
- IG-430 (due to fine grain) tends to differ from other isotropic grades at similar irradiation conditions (protons).
- Effects of proton irradiation on the physio-mechanical properties of IG-430 (Young's modulus, strength, dimensional stability, irradiation-induced growth) have shown to exhibit generally similar trends to those observed in nuclear graphite under neutron irradiation as it pertains to fractional change of Young's modulus and strength with increasing dose. Due to the inherent drawback, however, that during proton irradiation there exists lack of uniformity in the irradiation temperature, additional experiments are required to establish a direct neutron vs. proton comparison regarding changes with fluence.
- The dependence of strength and modulus evolution on proton fluence, including the effect on these properties of post-irradiation annealing was shown to exhibit similar trends to what has been observed for nuclear graphites under neutrons, particularly the reduction of strength above a fluence threshold (~10^{21} cm^{-2}) and only its partial recovery of modulus upon post-irradiation annealing.

The effects of energetic proton irradiation on the lattice structure of the IG-430 graphite have revealed the following:

- Similar to the observations made for graphites irradiated at low temperatures (<200 °C) IG-430 is shown to also experience the loss of long range structure above a critical fluence where it is also fragmented to smaller crystallites. This constitutes an important finding of the study in that such threshold proton fluence on graphite has also been observed in graphite under neutron irradiation at around a similar fluence level, ~5–6 10^{20} cm^{-2}, [31].
- The lattice parameter changes observed under protons exhibit similar trends to those reported for neutrons and other nuclear graphites for fluences ~2^{21} cm^{-2} and the temperature regime of the proton irradiations of the present study (up to ~210 °C). The trend indicated refers to the fact that the c-parameter increase in the temperature regime below ~200 °C increases disproportionally with lower irradiation temperatures.

Declaration of Competing Interest

The authors declare that they have no known competing financial interests or personal relationships that could have appeared to influence the work reported in this paper.

Supplementary materials[2]

Supplementary material associated with this article can be found, in the online version, at doi:10.1016/j.jnucmat.2020.152438.

References

[1] E. Kunimoto, T. Konishi, M. Eto, T. Shibata, Y. Katoh, Irradiation program for IG-110 and IG-430 graphites to evaluate its high fluence behavior and pre-irradiation sample size validation, in: Proceedings of the 13th International Nuclear Graphite Specialists Meeting, 2012 September 23-26.
[2] E. Kunimoto, M. Yamaji, T. Konishi, Y. Katoh, M. Snead, Irradiation program for IG-110 and IG-130 graphite for evaluation of high fluence behavior, in: Proceedings of the 15th International Nuclear Graphite Specialists Meeting, TECS-14058, Hangzhou, China, 2014.
[3] E. Kunimoto, J. Sumita, et al., Evaluation of material properties of IG-430 graphite for next generation high temperature gas-cooled reactor, in: Proceedings of the 16th International Nuclear Graphite Specialists Meeting, 2015.
[4] T. Shibata, et al., Interpolation and extrapolation method to analyze irradiation-induced dimensional change data of graphite for design of core components in very high temperature reactor (VHTR), J. Nucl. Sci. Technol. 47 (7) (2010) 591–598.
[5] S.-H. Chi, G.-C. Kim, Comparison of 3 MeV C + ion-irradiation effects between the nuclear graphites made of pitch and petroleum cokes, J. Nucl. Mater. 381 (1) (2008) 98–105.
[6] J.A. Vreeling, O. Wouters, J.G. van der Laan, Graphite irradiation testing for HTR technology at the high flux reactor in Petten, J. Nucl. Mater. 381 (2008) 68–75.
[7] Anne A. Campbell, Y. Katoh, M.A. Snead, K. Takizawa, Property changes of G347A graphite due to neutron irradiation, Carbon 109 (2016) 860–873.
[8] Anne A. Campbell, Gary S. Was, Proton irradiation-induced creep of ultrafine grade graphite, Carbon 77 (2014) 993–1010.
[9] M.C.R. Heijna, S. de Groot, J.A. Vreeling, Comparison of irradiation behaviour of HTR graphite grades, J. Nucl. Mater. 492 (2017) 148–156.
[10] M.I. Heggie, I. Suarez-Martinez, C. Davidson, G. Haffenden, Buckle, ruck and tuck: a proposed new model for the response of graphite to neutron irradiation, J. Nucl. Mater. 3 (2011) 413.
[11] M. Bogomilov, et al., Neutrino factory, Phys. Rev. ST Accel. Beams 17 (2014) 121002.
[12] Simos, et al., Proton irradiated graphite grades for a long baseline neutrino facility experiment, Phys. Rev. Accel. Beams 20 (2017) 071002.
[13] N. Simos, et al., 120 GeV neutrino physics graphite target damage assessment using electron microscopy and high-energy X-ray diffraction, Phys. Rev. Accel. Beams 22 (2019) 041001.
[14] N. Simos, et al., Irradiation damage studies of high power accelerator materials, J. Nucl. Mater. 377 (Part 1) (2008) 41–51.
[15] B.T. Kelly, The behavior of graphite under neutron irradiation, J. Vac. Sci. Technol. A4 (1986) 1171–1178.
[16] R. Taylor, et al., The mechanical properties of reactor graphite, Carbon 5 (1967) 519–553.
[17] B.T. Kelly, J.E. Brocklehurst, High dose fast neutron irradiation of highly oriented pyrolytic graphite, Carbon 9 (1971) 783.
[18] BT. Kelly, On the amorphization of graphite under neutron irradiation, J. Nucl. Mater. 172 (2) (1990) 237–238.
[19] Kelly, B. T., B. J. Marsden, K. Hall, D. G. Martin, A. Harper, and A. Blanchard. "Irradiation damage in graphite due to fast neutrons in fission and fusion systems." *IAEA Tecdoc* 1154 (2000).
[20] B.J. Marsden, "Irradiation Damage in Graphite. The Works of Professor B.T. Kelly." IAEA: N. p., 1996. Web. pp. 17-46.
[21] LL Snead, TD Burchell, Y. Katoh, Swelling of nuclear graphite and high quality carbon fiber composite under very high irradiation temperature, J. Nucl. Mater. 381 (1–2) (2008) 55–61.
[22] A. Burkholtz, "Irradiation Damage in Graphite," Report Prepared at the CEN, EUR 3056.e, 1966.
[23] N. Maruyama, M. Harayama, Neutron irradiation effect of thermal conductivity and dimensional change of graphite materials, J. Nucl. Mater. 195 (1992) 44–50.

[2] Aknowledgements: This research used The X-ray Powder Diffraction beamline of the National Synchrotron Light Source II, a U.S. Department of Energy (DOE) Office of Science User Facility operated for the DOE Office of Science by Brookhaven National Laboratory under Contract No. DE-SC0012704. This research used The X17B1 beamline of the National Synchrotron Light Source, a U.S. Department of Energy (DOE) Office of Science User Facility operated for the DOE Office of Science by Brookhaven National Laboratory under Contract No. DE-AC02-98CH10886.

[24] J-P. Bonal, et al., Graphite, ceramics, and ceramic composites for high-temperature nuclear power systems, MRS Bull. 34 (2009) 28–34.
[25] J. Eapen, et al., Early damage mechanisms in nuclear grade graphite under irradiation, Mater. Res. Lett. 2 (1) (2014) 43–50.
[26] H. Bridge, B.T. Kelly, B.S. Gray, Stored energy and dimensional changes in reactor graphite, in: Proceedings of the 5th Carbon Conference, 1961, pp. 289–316.
[27] D. G. Schweitzer, "Activation energy for single interstitials in neutron-irradiated graphite and the absolute rate of formation of displaced atoms," Phys. Rev., Vol. 128, No. 2, 1962.
[28] E. Kaxiras, K.C. Bandley, Energetics of defects and diffusion mechanisms in graphite, Phys. Rev. Letters 61 (23) (1988) 2693–2696.
[29] C.P. Ewels, R.H. Telling, A.A. El-Barbary, M.I. Heggie, P.R. Briddon, Metastable Frenkel pair defect in graphite: source of Wigner energy? Phys. Rev. Lett. 91 (2) (2003) 025505-1-4.
[30] A.V. Krasheninnikov, K. Nordlund, Ion and electron irradiation-induced effects in nanostructured materials, J. Appl. Phys. 107 (2010) 071301.
[31] W. Bollmann, Electron-microscopic observations on radiation damage in graphite, Phil. Mag. 5 (54) (1960) 621–624.
[32] W.T. Eeles, Diffuse diffraction phenomena from neutron-irradiated graphite single crystals, ACA 24 (6) (1968) 688–689.
[33] Gittus, Creep, Viscoelasticity and Creep Fracture in Solids, Wiley, 1975.
[34] C. Hubert, et al., "High Resolution Synchrotron X-ray Diffraction of Swift Heavy Ion Irradiated Graphite," PNI-INHOUSE-EXP-39, GSI SCIENTIFIC REPORT, 2012.
[35] T. Shibata, et al., Oxidation damage evaluation by non-destructive method for graphite compounds in high temperature gas-cooled reactor, J. Solid Mech. Mater. Eng. 2 (1) (2008) 166–175.
[36] S.-H. Chi, G.-C. Kim, Mrozowski cracks and oxidation behavior of IG-110 and IG-430 nuclear graphites, Transactions of the Korean Nuclear Society Spring Meeting Chuncheon, Korea, 2006 May 25-26.
[37] G.S. Was, et al., Emulation of reactor irradiation damage using ion beams, Scr. Mater. 88 (1) (2014) 33–36.
[38] L.F. Mausner, et al., The design and operation of the upgraded BLIP facility for radionuclide research and production, Int. J. Radiat. Appl. Instrum. Part A Appl. Radiat. Isot. 41 (4) (1990) 367–374.
[39] https://www.toyotanso.com/Products/application/atomic-nuclear.html.
[40] https://www.toyotanso.com/Products/Special_graphite/data.html.
[41] T.T. Böhlen, F. Cerutti, M.P.W. Chin, A. Fassò, A. Ferrari, P.G. Ortega, A. Mairani, P.R. Sala, G. Smirnov, V. Vlachoudis, The FLUKA code: developments and challenges for high energy and medical applications, Nucl. Data Sheets 120 (2014) 211–214.
[42] A. Ferrari, P.R. Sala, A. Fasso, J. Ranft, U. Siegen, *FLUKA: a multi-particle transport code* (No. SLAC-R-773), Stanford Linear Accelerator Center (SLAC), 2005.
[43] Mokhov, N.V. and James, C.C. *The MARS code system user's guide version 15 (2016)*. No. FERMILAB-FN-1058-APC. Fermi National Accelerator Lab.(FNAL), Batavia, IL (United States), 2017.
[44] LS-DYNA, Version 9.71, Livermore Software Technology Corp. (LSTC), 2007.